A Comprehensive Analysis of the Thermal Elimination Reaction in a Poly(*p*-phenylene vinylene) Precursor

Hiren V. Shah and Georgia A. Arbuckle*

Department of Chemistry, Rutgers, The State University of New Jersey, Camden, New Jersey 08102

Received July 14, 1998; Revised Manuscript Received January 7, 1999

ABSTRACT: Sulfonium precursor routes are the most popular synthetic routes to light-emitting poly(*p*-phenylene vinylene) (PPV) thin films. These routes involve a high-temperature solid-state thermal elimination reaction which yields PPV from its water-soluble precursor. The quality of PPV and hence its ultimate properties have a strong dependence on the polymerization parameters and thermal elimination conditions. The elimination reaction remains less understood. In this report, we have qualitatively and quantitatively analyzed the thermal elimination reaction using TGA, DSC, MTGA, TG-IR and transmission IR. The qualitative analysis focuses on identification of the underlying reactions and establishing the reaction sequence and reaction mechanisms. The quantitative analysis, on the other hand, focuses on the determination of the kinetic parameters of these reactions. The effect of heating rate and reaction environment on the luminescent properties of PPV have also been investigated.

1. Introduction

Poly(*p*-phenylene vinylene) (PPV) is an electroactive polymer which exhibits many optoelectronic properties such as electrical conductivity,[1] electroluminescence,[2] photoluminescence,[3] and photoconductivity.[4] Like most conjugated polymers, PPV also has processibility problems because of its inherent insolubility and infusibility. Therefore, a preferable synthetic route to PPV involves the preparation of a soluble precursor polymer which can be cast into films and then be converted into PPV films via a solid state thermal elimination reaction. This thermal reaction is normally carried out under either vacuum or an inert atmosphere. It has been suggested by several workers[5−9] that the formation of defects in PPV occurs during this thermal conversion. These defects limit the conjugation length and thereby affect the charge transport, conductivity, and luminescence in this polymer.[10]

The thermal conversion of a sulfonium precursor has been investigated in the past with the aid of several different techniques including thermogravimetry (TGA),[11,12] differential scanning calorimetry (DSC),[11−13] thermogravimetry−mass spectroscopy (TG−MS),[14,15] thermogravimetry-infrared spectroscopy (TG-IR),[14] and even X-ray diffraction (XRD).[16] Earlier studies[11,17,18] were performed on a PPV precursor synthesized from a dimethylsulfonium salt. A derivative of this monomer with a cyclic tetrahydrothiophenium (THT) pendant group yields PPV with higher average conjugation length.[5,9] Several recent reports[12−14] have focused on the elimination reaction in the THT precursor polymer. Unfortunately, these studies are not in agreement because the reaction is quite complex with several different mechanisms operating either sequentially or simultaneously.

In the current study, we have identified the transition states and reaction mechanisms during the elimination reaction in a PPV precursor using DSC and TGA in conjunction with infrared spectrophotometry. The TG−IR approach enables measurement of reaction rates by TGA and the reaction byproducts by IR spectrophotometry. This technique is also known as evolved gas analysis or EGA. Thermal conversion of the precursor film was also monitored by in-situ IR transmission spectroscopy to thoroughly understand the reaction.

From the TGA data, we have determined the kinetic parameters of the reaction using two different methods. In the first method, also the traditional method, the thermal conversion was carried out at several different heating rates. This method, however, operates under the assumption that a single reaction operating under a single mechanism controls the entire temperature range. The limitation of the traditional method can be circumvented by applying a recently developed modulated TGA (MTGA) approach which uses a sinusoidal temperature modulation on the underlying traditional heating profile. This method has also been employed in the current study to determine the kinetic parameters of the intermediate reactions. The scope of this investigation has been further extended to study the effect of heating rate on the luminescence of the polymer.

2. Nonisothermal Kinetics

2.1. Traditional Approach. Polymer thermogravimetric kinetics[19] have been discussed in detail by Doyle.[20] He has shown that the fraction of mass volatilized, dC, in temperature interval, dT, is related to the heating rate, β, by the following equation

$$\frac{dC}{dT} = (A/\beta)f(C)^{-E/RT} \tag{1}$$

where

$A =$ preexponential factor of the Arrhenius equation.

$f(C) =$ function of the degree of conversion, whose specific form depends on the order of the reaction.

Equation 1 may be integrated to obtain

$$F(C) = \left(\frac{AE}{\beta R}\right)p(x) \tag{2}$$

where

10.1021/ma981108q CCC: $18.00
Published on Web 02/10/1999

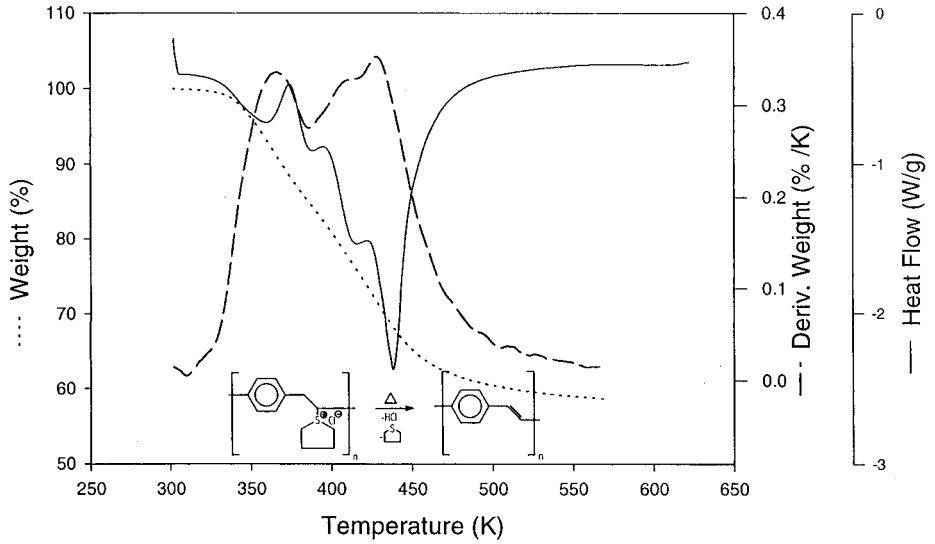

Figure 1. DSC plot of PPV precursor from ambient temperature to 620 K at a heating rate of 3 K/min (solid); TG (short dash)/ DTG (long dash) plot from ambient temperature to 570 K at a heating rate of 3K/min; schematic representation of the elimination reaction (inset).

$$F(C) = \int_0^c \frac{dC}{f(C)}$$

$$x = E/RT$$

$$p(x) = [e^x/x] - \int_\infty^\infty (e^{-u}/u)\, du$$

The function $p(x)$ can be obtained using standard integral tables.

Using eq 1 as the starting point, Flynn and Wall[21] have proved that at a constant degree of conversion, C, the activation energy, E, of a reaction is related to the heating rate, β, and the temperature, T, by the following equation:

$$E = -(R/b)\frac{\Delta \log \beta}{\Delta\, 1/T} \qquad (3)$$

where b is a constant with a value of 0.475 K^{-1}. The raw value of E can be obtained from the slope of the log β versus $1/T$ plot. The refined value of the activation energy is calculated by an iterative process involving successive approximations of the constant, b, and the activation energy, E.

If the activation energy and the order of the reaction are known, the preexponential factor, A, can be determined from eq 2.

2.2. Modulated TGA Approach. As mentioned earlier, in MTGA, a steadily increasing but sinusoidally oscillating temperature program is applied to the sample. This sinusoidally temperature-varying program in TGA produces a change in the response of the test specimen in terms of its rate of weight loss. This rate of weight loss profile can be used to obtain the kinetic parameters.

This approach was first described in 1968 by Flynn[22] but has been very recently implemented using a TGA.[23,24] In this method, the activation energy is described by the following equation:

$$E = \frac{R(T^2 - \alpha^2)}{2\alpha} \ln\left(\frac{d\alpha_1}{d\alpha_2}\right) \qquad (4)$$

where

T = average temperature.

α = temperature amplitude.

$d\alpha_1/d\alpha_2$ = ratio of the maximum and minimum rate of weight loss taken at adjacent half-cycles of the sine wave.

The values of T, α, and the differential component in the above equation are obtained by deconvolution of the oscillatory temperature program and the resultant oscillatory rate of weight loss using a real-time discrete Fourier transform.

Equation 4 is essentially "model free" because it does not rely on a kinetic function for its calculation. The other benefits of this technique include short experiment time and real-time availability of the kinetic data during the progress of the reaction.

3. Experimental Section

PPV films were synthesized by base-induced polymerization of *p*-xylylidiene tetrahydrothiophenium chloride as suggested by Wessling and Zimmerman.[25] The synthetic procedure has been described in detail elsewhere.[26] For the TGA−IR analysis, a TA Instruments 2050 TGA was connected to a Bio-Rad FTS-6000 IR system via a heated transfer line maintained at 523 K. Differential scanning calorimetry was carried out using a TA Instruments 2920 DSC. All of the experiments were performed in a nitrogen atmosphere. The TGA−IR experiments were repeated at five different heating rates (1, 2, 3, 5, and 7 K/min). The DSC experiment was performed at a heating rate of 3 K/min. TA Instruments TGA kinetic software was used to determine kinetic parameters. For the MTGA study, a TA Instruments 2950 Hi-Res TGA delivering a temperature modulation of 10 K and a modulation period (frequency) of 180 s with an underlying heating profile of 2 K/min was employed. A Harrick Scientific HTC 100 heated transmission IR cell was used for in-situ transmission infrared studies. The cell was controlled by an automatic temperature feedback controller (AT-30D) and was water cooled to prevent damage to the cell windows (KBr). The cell was continuously purged with argon to maintain an inert atmosphere within the cell. Photoluminescence spectroscopy was carried out using a Perkin−Elmer SL 50 spectrophotometer at an excitation wavelength of 288 nm and a scan rate of 200 nm/min. Photoacoustic spectra were obtained using an MTEC 300 photoacoustic cell mounted in the Bio-Rad IR spectrometer.

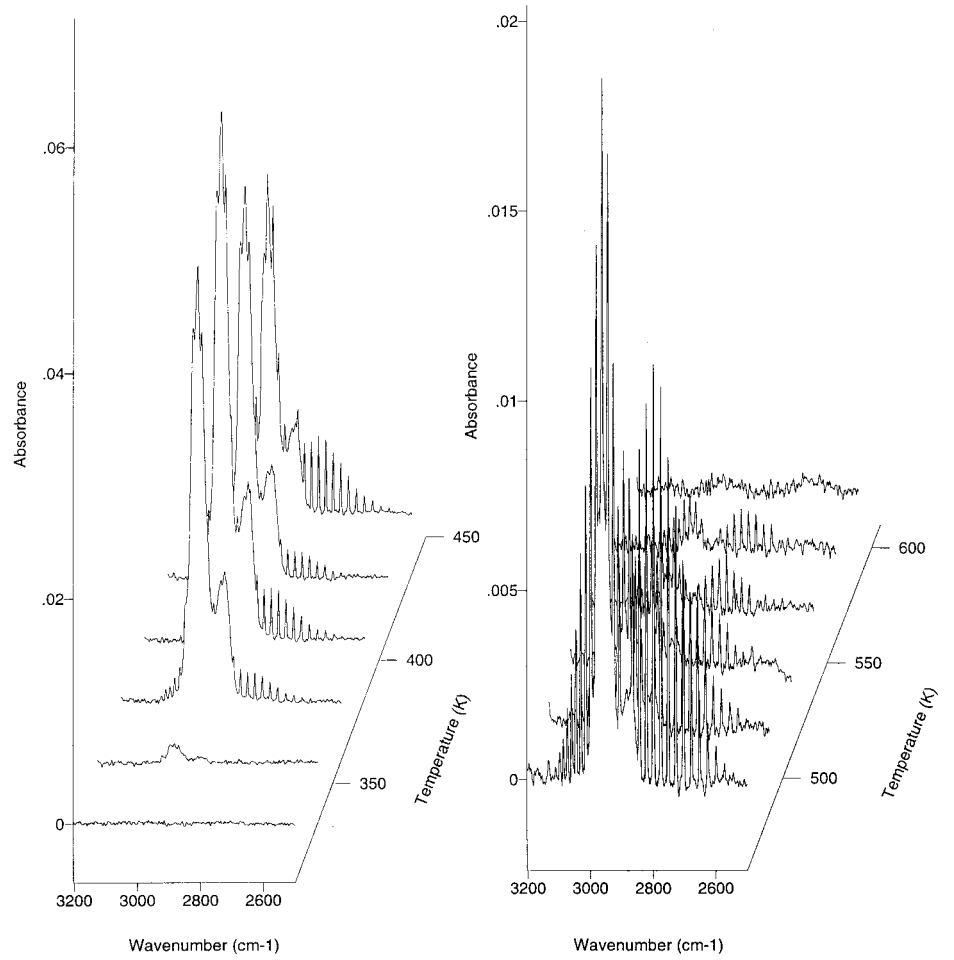

Figure 2. Three-dimensional temperature−frequency−intensity IR plots of the reaction byproducts.

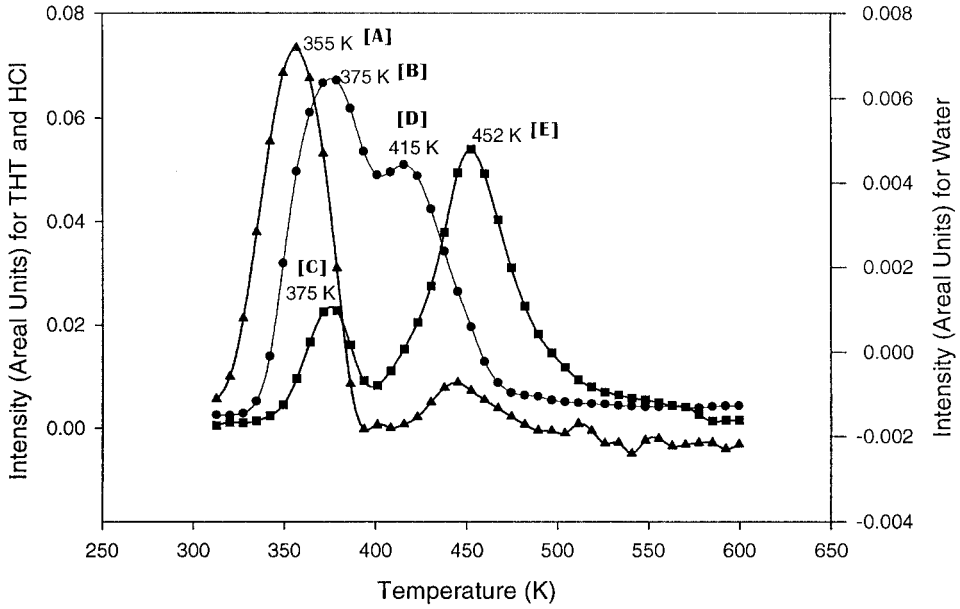

Figure 3. EGA chromatograms of (●) THT, (■) HCl, and (▲) water.

4. Results and Discussion

4.1. Qualitative Aspects. The thermal elimination reaction in the PPV precursor is shown in Figure 1 as an inset. The reaction involves the elimination of THT groups and hydrochloric acid (HCl) from the precursor backbone to yield vinylene groups.

The DSC plot of the PPV precursor when heated from ambient temperature to 620 K at a rate of 3 K/min is shown in Figure 1. The plot shows four distinct endotherms with minima at 359, 388, 415, and 438 K. From these results, it can be inferred that there are at least four subprocesses occurring during the elimination

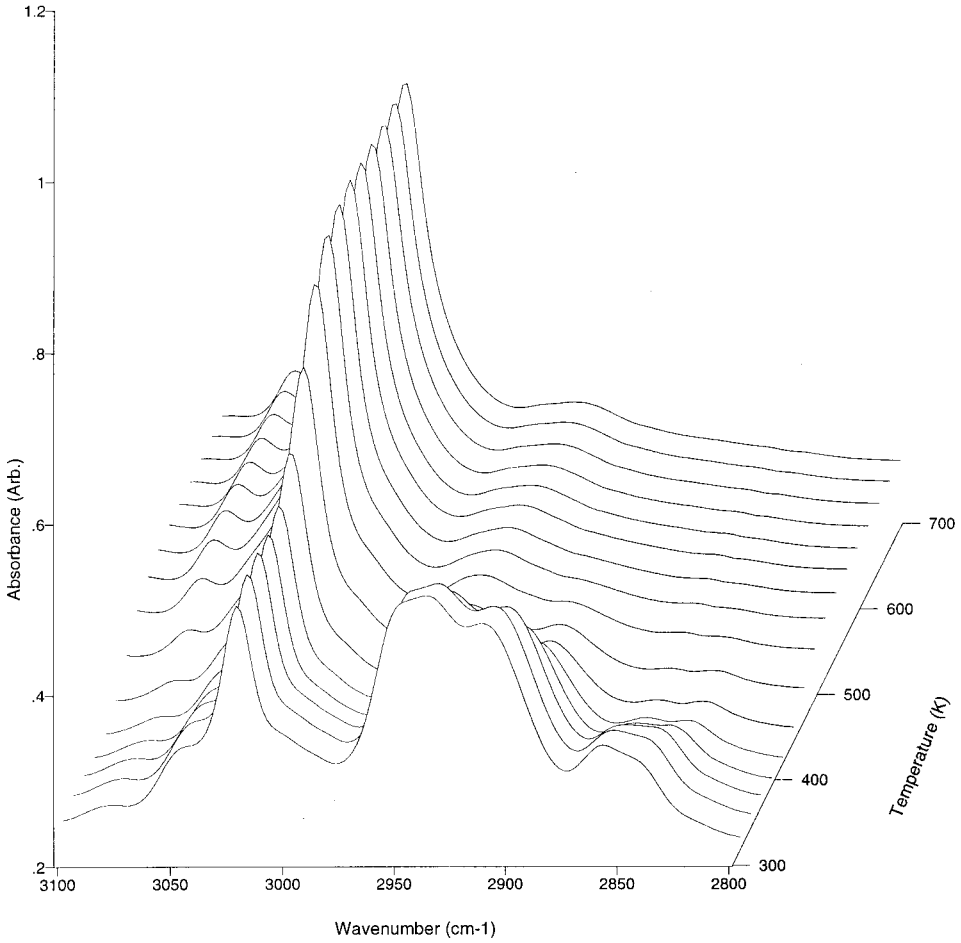

Figure 4. Three-dimensional temperature−frequency−intensity transmission IR spectral plots in the 3200−2800 cm^{-1} region.

reaction. It should be noted that the sample is continuously losing mass during the entire experiment. Therefore, no meaningful quantitative information can be obtained from DSC analysis.

The corresponding thermal weight-loss curve, known as a thermogram or TG, also operated at a heating rate of 3 K/min and shows an overall weight loss of about 40%, as illustrated in Figure 1. On careful examination, one can notice slope changes in the thermogram during the course of the reaction. The derivative of the thermogram with respect to time, also known as a differential thermogram or DTG, indeed shows three inflection points at 366, 410, and 428 K (which correspond to weight losses of 91, 78, and 72% respectively), thereby confirming the presence of several different processes. The overall weight loss is ∼40%; it may be noted that the precursor continuously converts to PPV at room temperature and that residual water is present in the precursor, as confirmed by IR spectra of the evolved gas products.

The IR spectra of the reaction byproducts, during an EGA scan, are plotted with respect to temperature in Figure 2. As the reaction begins, two overlapping bands at 2957 and 2972 cm^{-1} emerge. These bands have been assigned to C−H stretches of two different types of carbon atoms in THT. One also sees the evidence of vibration−rotation bands due to HCl (3100−2800 cm^{-1}) in the initial stages of the reaction. The intensity of the THT bands slowly diminishes as the reaction proceeds. The HCl bands, on the other hand, reappear and continue to grow in intensity as the THT bands are fading. A clear picture emerges if one looks at the THT, HCl, and water chromatograms shown in Figure 3. The chromatograms distinctly show that water evolves right from the start of the reaction with a maximum at 355 K [A] most likely because of the presence of residual quantities of unbound water. The THT chromatogram on the other hand is bimodal, with peaks at 375 [B] and 415 K [D]. The HCl chromatogram is also bimodal with a relatively smaller peak at 375 K [C], which coincides with the first peak in the THT chromatogram, indicating that these two processes are related. The second peak, which is more intense than the first one, occurs at 452 K [E]. This peak, incidentally, does not coincide with the second peak of the THT chromatogram. Even though there is some degree of overlap between the HCl and the THT evolution, elimination of THT and HCl seems to occur via two different processes. Therefore it appears that there is an intermediate transition state during the elimination in which the polymer still retains chlorine even though it has lost most of the THT species.

The analysis so far clearly indicates the existence of several processes during the elimination reaction. These are (1) Removal of small quantities of water. (2) Elimination of THT by two different processes, the first of which is accompanied by the evolution of small quantities of HCl. (3) Elimination of HCl, also by two different processes, the first of which is coincident with the THT elimination, as mentioned above, and the second, occurring toward the end of the elimination reaction, which is relatively independent from the THT elimination.

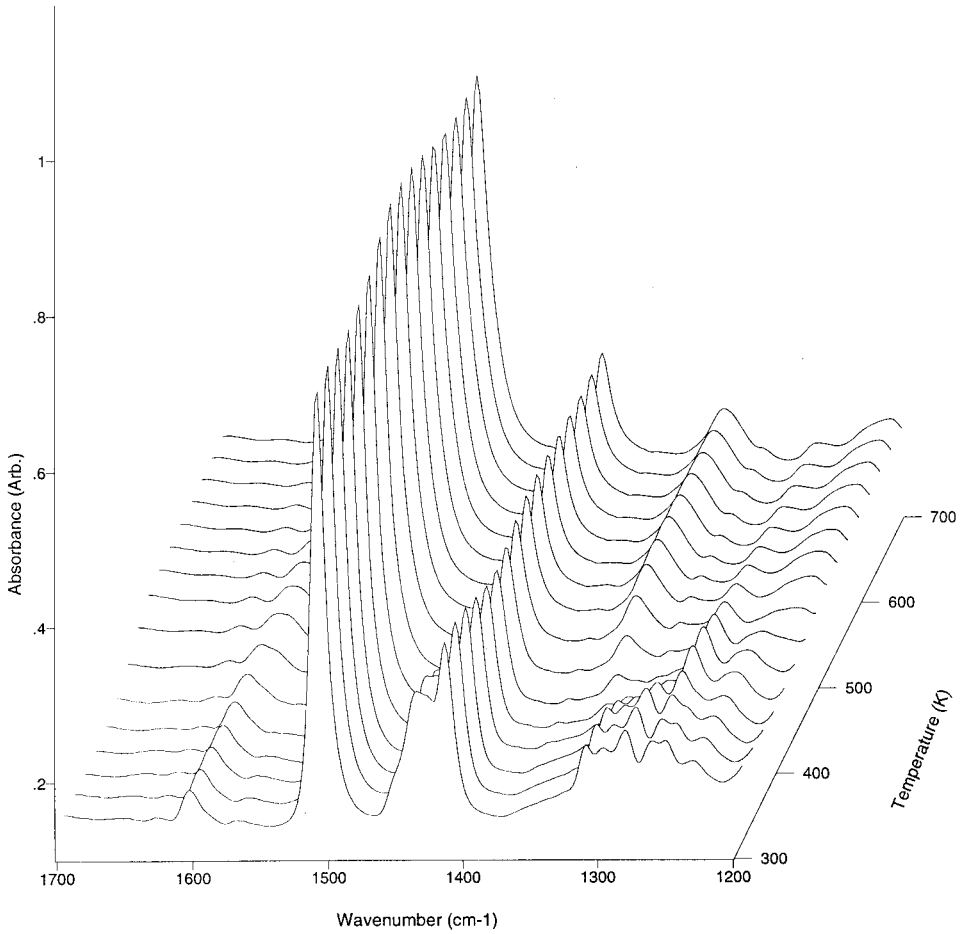

Figure 5. Three-dimensional temperature−frequency−intensity transmission IR spectral plots in the 1700−1200 cm^{-1} region.

All of the aforementioned processes are easily observed with the different techniques applied in our studies. Even though each of these analytical tools monitors widely differing physical properties to achieve the results, the mean temperature value for each process shows a surprisingly good mutual agreement (compare Figures 1 and 3).

To gain a deeper understanding of the reaction mechanism, infrared transmission spectra of the polymer film were recorded in situ during the elimination reaction at a heating rate of 5 K/min. The results are presented as a series of spectral plots at regular time intervals, as shown in Figures 4−6. Figure 4 shows the 3200−2800 cm^{-1} region exhibiting several C−H stretching vibrations. In this region, the evolution of the vinylene (sp^2) C−H stretching band at 3024 cm^{-1} can be observed while several aliphatic (sp^3) C−H stretches (2944, 2915, 2860 cm^{-1} etc.), due to THT and partially aliphatic backbones, diminish in intensity.

In the first section of the fingerprint region from 1700 to 1200 cm^{-1}, as shown in Figure 5, relatively little activity is observed. The C−C ring stretches between 1550 and 1400 cm^{-1} show negligible changes. However, the peaks in the 1350−1200 cm^{-1} region exhibit some intensity changes and frequency shifts.

In the second section of the fingerprint region (1200−400 cm^{-1}), as shown in Figure 6, the vinylene C−H bend at 963 cm^{-1}, the phenylene C−H bend at 837 cm^{-1}, and the phenylene ring bend at 555 cm^{-1} increase in intensity. On the other hand, many of the small peaks (630, 657, and 920 cm^{-1}) due to pendant group vibrations disappear during the course of the reaction.

Again, for more clarity, chromatograms of several peaks of interest can be constructed by integrating the area underneath each peak (because there are peak shifts involved, peak area was used as a measuring parameter rather than peak height). Figure 7 shows the chromatograms of several peaks as indicated. Please note that the plots in Figure 7 have been offset and arbitrarily scaled in the *y*-direction for clarity. As expected, the aliphatic C−H trace (Figure 7a) shows a sharp decline, and the vinylene C−H stretch (Figure 7b) and C−H bend (Figure 7c) traces exhibit a steep incline. However, the drop in the aliphatic C−H chromatogram does not coincide with the onset of the vinylene C−H chromatogram as observed in Figure 7. The delayed evolution of the vinylene bands indicates that the high intensity of aliphatic C−H bands in the PPV precursor is predominantly due to THT, because THT is found to evolve first during the elimination (Figure 3), and more importantly, it proves that backbone conjugation does not occur immediately after the elimination of THT.

The peak at 630 cm^{-1} in the precursor film exhibits a very different behavior, which is evident from its chromatogram, as shown in Figure 7d. The intensity of this chromatogram, steady at first, increases while the intensity of the aliphatic C−H chromatogram decreases, and then it starts to decrease again, as the intensity of the vinylene bands start to increase and the 630 cm^{-1} peak eventually approximates zero intensity. This 630 cm^{-1} peak may be assigned to the *cis*-vinylene C−H vibration.[18] Therefore, it follows that the elimination of THT is accompanied by creation of cis linkages which

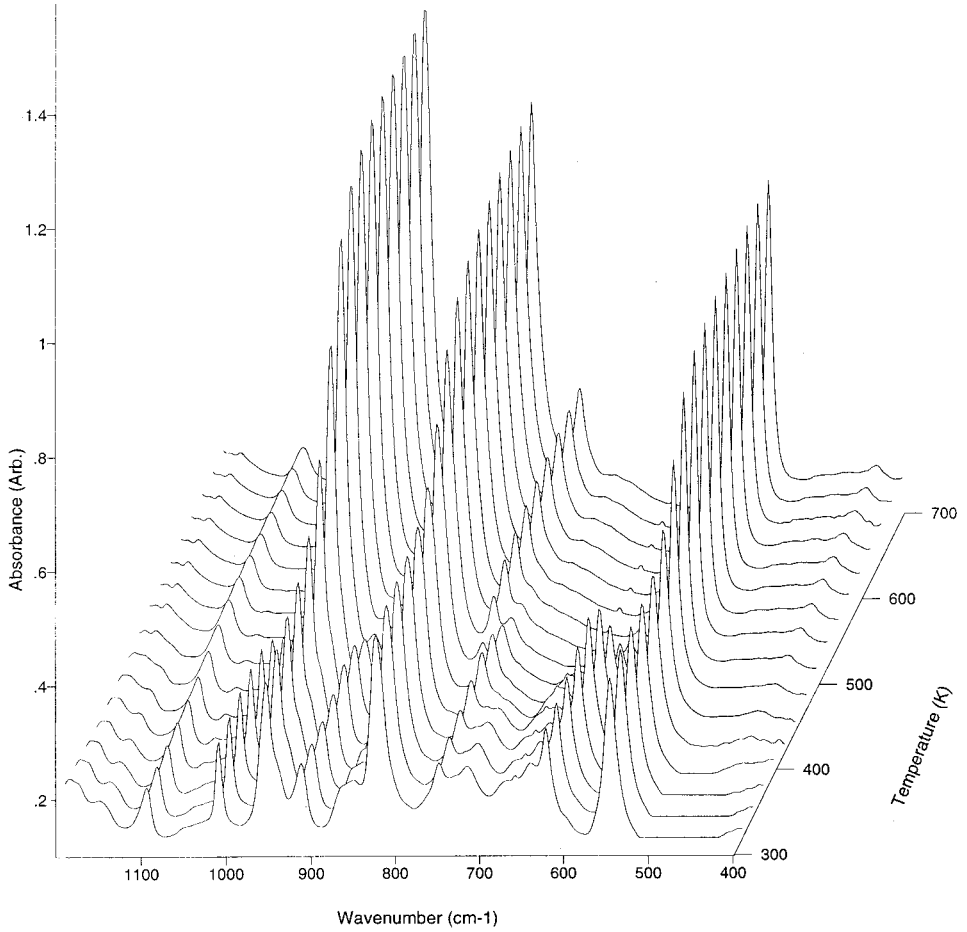

Figure 6. Three-dimensional temperature−frequency−intensity transmission IR spectral plots in the 1200−400 cm^{-1} region.

eventually isomerize to thermodynamically stable trans linkages.

Another peak of interest is the phenylene ring bend at 555 cm^{-1}, which also shows a unique behavior as seen in Figure 7e. The chromatogram of this peak also increases in intensity with the progress of the reaction; however, the intensity distribution is bimodal. The first increase in intensity coincides with the elimination of THT, whereas the second one coincides with the elimination of HCl. This behavior can be understood by considering the intermolecular and possibly intramolecular steric hindrance to the ring bending due to the presence of the bulky THT group and chloride ions as pendent units on the backbone.

On the basis of all of the experimental evidence, it can be inferred that the elimination reaction in the PPV precursor is extremely complex, involving at least two elimination processes and exhibiting a strong dependence on the stereochemical structure of the precursor. The structure of the precursor backbone may be envisaged to possess three limiting conformations, as shown in Figure 8. Thermodynamically, conformation A is more stable than B and C; however, the existence of the latter two conformations at high temperatures seems likely. The conformation of the THT groups and proton, can be antiperiplanar or synperiplanar or both, as indicated in Figure 8. Each of the conformations A−C can give rise to cis or trans linkages or both in the final polymer, as shown in the figure. EGA chromatograms in Figure 3 provide evidence of an E2 mechanism at low temperatures by simultaneous release of THT and HCl. Because E2 elimination is stereoselective and prefers antiperiplanar conformations of the leaving groups,[27] it can give rise to a mix of cis and trans configurations in this case (refer to Figure 8). Indeed, that is precisely what is observed in the transmission chromatograms of Figure 7 at marker I on traces b−d; both the trans vinylene stretch and the trans and cisvinylene bends change in intensity. Relative abundance of HCl at peaks [C] and [E] in Figure 3 suggests that an E1 mechanism might also be dominating the reaction at high temperatures, whereas E2 dominates in the low-temperature region.

At high temperatures, on the other hand, the elimination seems to occur solely via an E1 mechanism. In an E1 mechanism, the elimination will occur via the formation of an intermediate carbonium or carbocation, which in this case will be resonance stabilized and therefore can be quite long-lived (refer to Figure 9). The longevity of the carbonium ion would imply an increase in the cis configuration,[14,27] which is also readily observed experimentally (marker II in Figure 7d). This hypothesis is also supported by the fact that no evidence of C−Cl bonding could be found in the transmission IR. The final step in the elimination reaction, therefore, is the nucleophilic attack of a base (chloride ion) on the aliphatic carbon and the release of HCl. The HCl elimination also sees a sharp decline in the cis linkages (marker III in Figure 7) most likely occurring via a cis-to-trans isomerization process, as shown in Figure 9. The isomerization occurs simultaneously with an increase in trans linkages (Figure 7b,c) as expected. It is interesting to note that the bromide tetrahydrothiophenium chloride undergoes complete elimination[28] at

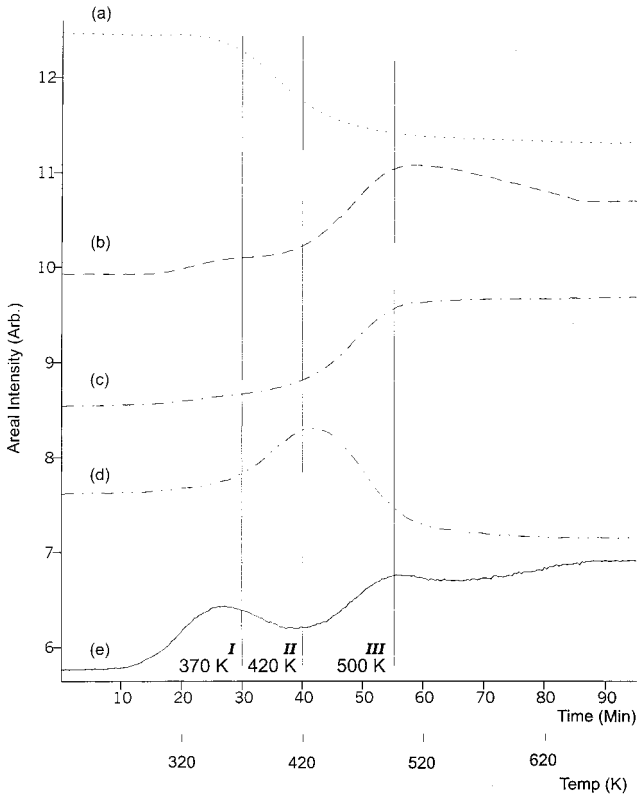

Figure 7. Chromatograms of several transmission IR peaks of the polymer during the elimination reaction: (a) aliphatic C−H stretch (2800−2960 cm^{-1}), (b) *trans*-vinylene C−H stretch (3024 cm^{-1}), (c) *trans*-vinylene C−H bend (965 cm^{-1}), (d) *cis*-vinylene C−H bend (630 cm^{-1}), and (e) phenylene ring bend (555 cm^{-1}).

Newmann Projections of Precursor Conformations	Possible Leaving-Group Conformations	Resulting Configurations in PPV
(A) 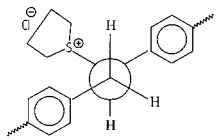	anti-periplanar & syn-periplanar	trans-linkage
(B) 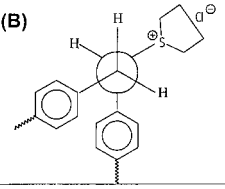	syn-periplanar	cis-linkage & trans-linkage
(C) 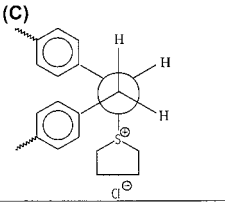	anti-periplanar & syn-periplanar	cis-linkage

Figure 8. Representation of the possible conformations in the PPV precursor.

about 100 °C, which is much lower than the corresponding temperature observed for the chloride polyelectrolyte, as noted here. This may be due to the lower electronegativity of bromine, and consequently, it acts as a better leaving group.

Our conclusion that both an E1 and E2 mechanism may be operating with the shift from E2 to E1 being dependent on reaction temperature and stereochemistry of the polymer is to a limited extent in agreement with a study by Massardier et al.[12] Schlenoff and Wang[14] have reported an E2 mechanism, and Halliday et al.[13] have reported an E1 mechanism. This is now understandable in light of the fact that both mechanisms are operative.

4.2. Determination of Kinetic Parameters

4.2.1. Traditional Approach. The determination of kinetic parameters is based on eqs 1−3. As mentioned previously, the traditional method requires the reaction to be carried out at several different heating rates. It was experimentally observed that more reliable results were obtained when the heating rate was maintained below 10 K/min. We, therefore, chose the heating rates of 1, 2, 3, 5, and 7 K/min. Several such sets of experiments were carried out, and the final values of the kinetic parameters reported in this article are the arithmetic means. However, the plots shown in this section are obtained from a typical run.

Detailed qualitative analysis of the reaction, described in the previous section, reveals that the reaction proceeds in at least two or more steps. Because of the limitations of the traditional method, we shall focus our attention only on the initial 25% weight-loss (380−400 K) which is associated primarily with the elimination of THT. The MTGA approach, on the other hand, will provide the activation energies for the higher weight-loss (or higher temperature) regions. To determine the activation energy for the first step, absolute temperatures at a constant conversion were determined for each thermogram in Figure 10. Conversion levels of 5, 10, 15, 20, and 25% were chosen for the first step, as shown in Figure 10.

A plot of the logarithm of heating rate against the inverse of the absolute temperature is obtained for each conversion level, as shown in Figure 11. The slope of each of the parallel straight lines, as expected from eq 3, in Figure 11 is a measure of the activation energy for the process. The slope, however, gives only an approximate value of the activation energy. A more refined value is obtained after performing an iterative process, as mentioned earlier. Knowledge of the activation energy permits calculation of the function $p(E/RT)$ for each point in Figure 11. Consequently, a plot of heating rate versus $p(x)$, where $x = E/RT$, can be constructed. If the order of the reaction is known, then the preexponential factor, A, can be determined for each conversion level using eq 2. Thus, the rate constant, k_1, associated with the elimination of THT, as shown in Figure 9, can be computed at any given temperature using the Arrhenius equation. Consequently the half-life of the precursor can also be predicted. As shown in Figure 12, the precursor half-life, which is only a few days at room temperature (300 K), can be considerably enhanced to almost a year by storing it at 273 K. The prediction of the half-life, or the shelf life of the precursor or both may be very important during mass production of the precursor for device applications and more importantly for the potential photolithography and photoresist applications because of the sensitivity of the precursor to UV light.[2]

Table 1 summarizes the arithmetic means of the activation energies and the preexponential factors of

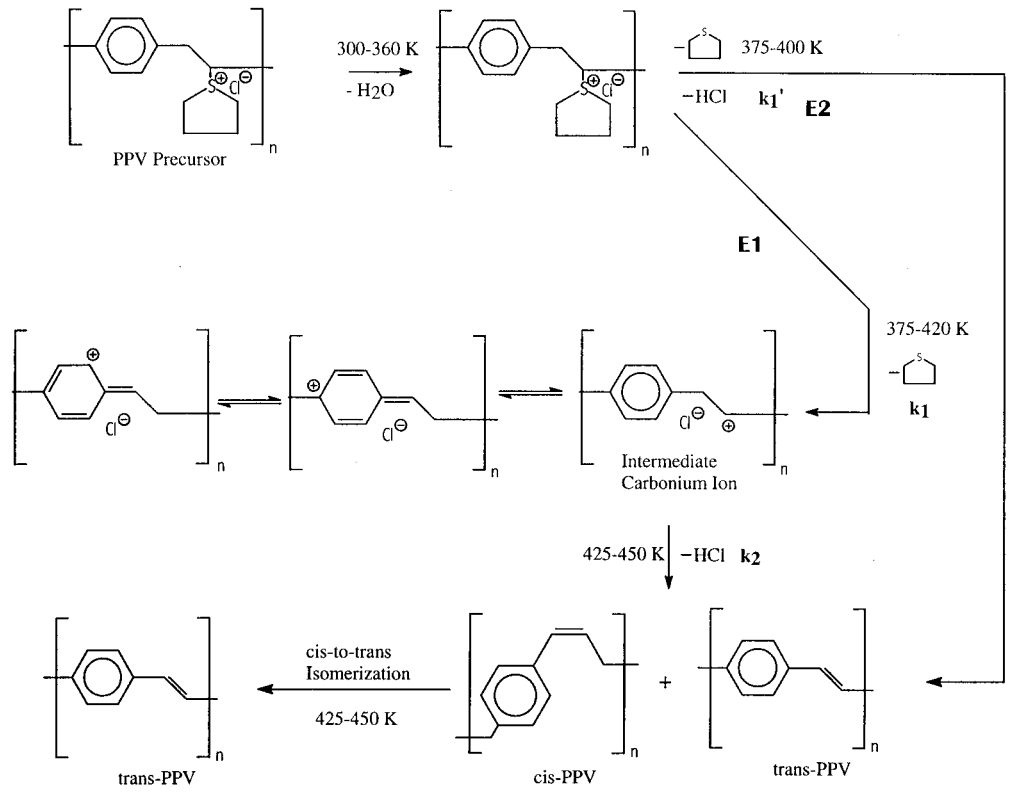

Figure 9. Proposed thermal elimination reaction sequence in the PPV precursor.

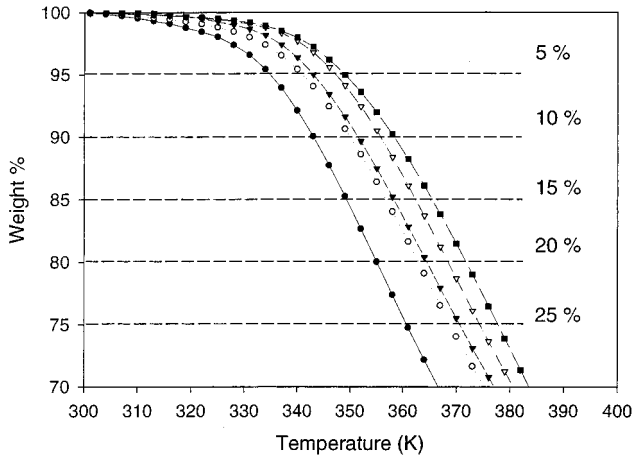

Figure 10. Thermograms at the heating rates of (●) 1 K/min, (○) 2 K/min, (▼) 3 (K/min), (▽) 5 K/min, and (■) 7 K/min showing the chosen conversion levels.

Table 1. Kinetic Parameters Determined at Various Conversion Levels

conversion, %	activation energy, kJ/mol	log (preexponential factor), min^{-1}
5	128	19
10	136	19
15	132	20
20	126	19
25	132	18

several such experiments. The results shown in Table 1 have been experimentally verified by confirming the 60 min half-life temperatures. The 60 min half-life temperature, at a given conversion level, is the temperature at which the material maintained for 1 h would register a weight loss equivalent to 50% of the conversion level.

4.2.2. Modulated TGA Approach. Earlier it was mentioned that MTGA allows the determination of activation energy values in real-time in a single scan. It also allows for unambiguous computation of activation energies for a multistep reaction such as this one. Figure 13 shows the thermogram from ambient temperature to 550 K along with the applied temperature modulation and computed activation energy values. When the rate of weight loss is low, the values of the activation energies are unrealistically high, and therefore, those values have been eliminated from the figure. As shown in Figure 13, the activation energies associated with the first two transitions (within initial 25% of weight loss), which are mainly due to the elimination of THT, are in the vicinity of 110 kJ/mol. This value agrees within experimental error with that obtained from the traditional approach (refer to Table 1). It also shows that the two steps associated with the elimination of THT have almost the same activation energy. The final step of the reaction, which is linked to the elimination of HCl, has a significantly higher activation energy, in the vicinity of 170 kJ/mol. Thus, the use of a combination of standard thermogravimetry and modulated thermogravimetry has made it possible to approximate the activation energies at different stages of the elimination reaction.

4.3. Effect of Heating Rate on Photoluminescence. Because light emission from PPV may prove to be one of its most useful applications, some attention has been devoted to studying the effect of heating rate on the luminescent properties of PPV. It has been suggested that the use of a reducing atmosphere, such as a mixture of an inert gas with hydrogen, during thermal elimination reduces the number of carbonyl defects significantly and thereby improves the luminescent properties.[6,7] Therefore, we have tried to encompass this particular aspect as well, by carrying out the

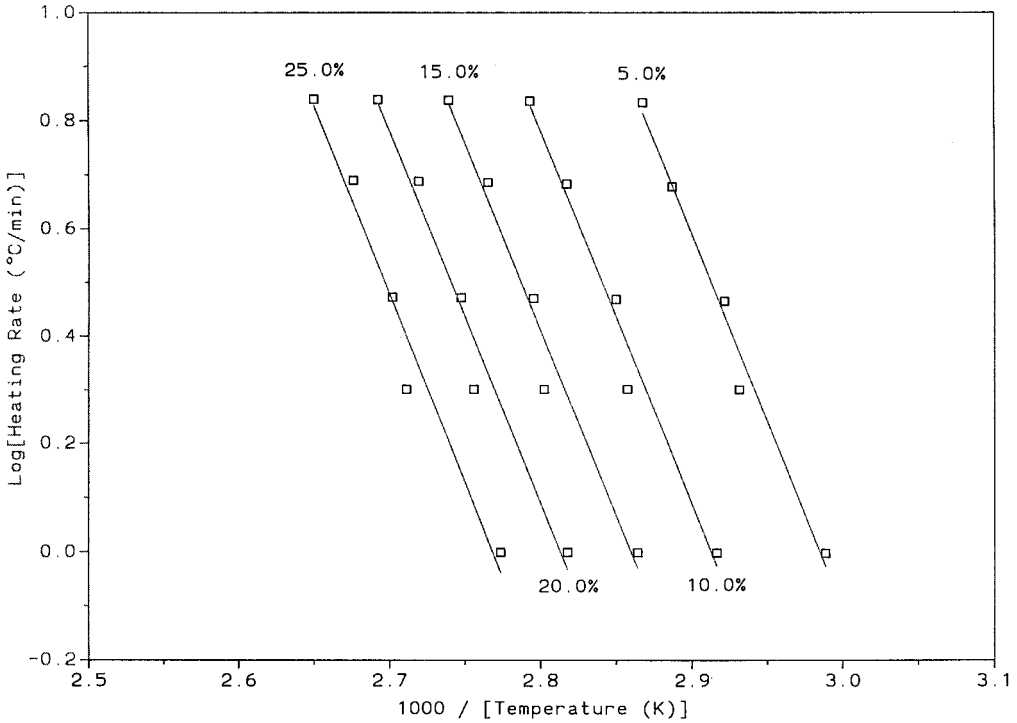

Figure 11. Plots of logarithm of heating rate versus inverse of absolute temperature at conversion levels of 5, 10, 15, 20, and 25%.

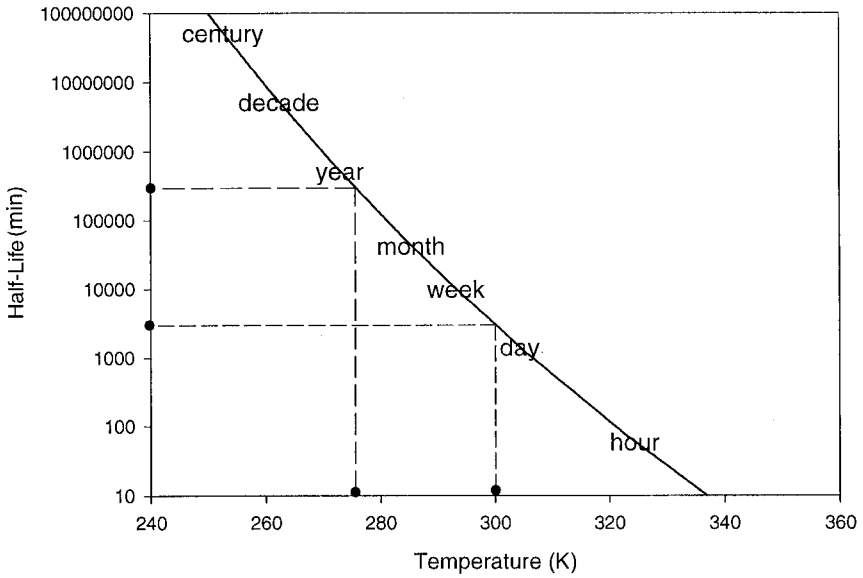

Figure 12. Half-life profile of the PPV precursor with respect to the storage temperature based on the first step of the elimination reaction.

reaction in the presence of a regular inert atmosphere containing pure nitrogen and a reducing inert atmosphere containing forming gas (95% argon + 5% hydrogen) at several different heating rates. The samples have also been investigated spectroscopically by using photoacoustic IR spectroscopy to detect the concentration of oxygen-containing species.

Figure 14 shows the effect of heating rate and the reaction atmosphere on luminescence. As the heating rate is reduced, a corresponding increase in luminescence is observed. On the other hand, using a reducing atmosphere also yields improved luminescence. As seen from Figure 14, the polymer converted with a heating rate of 10 K/min in a reducing atmosphere exhibits more luminescence than that converted with a heating rate of 5 K/min in a normal inert atmosphere. Similarly, the luminescent efficiency of the PPV synthesized at a heating rate of 20 K/min in a reducing atmosphere is higher than that synthesized at a heating rate of 10 K/min in a normal inert atmosphere. Therefore, it can be said that the quality of the inert gas atmosphere has a greater impact on the luminescent properties of PPV than the heating rate applied during the thermal conversion. Consequently, no evidence of an increased concentration of carbonyl defects was observed spectroscopically on increasing the heating rates and with the same atmospheric conditions. However, a clear indication of a decrease in carbonyl is obtained when a reducing atmosphere was used instead of the regular inert atmosphere.

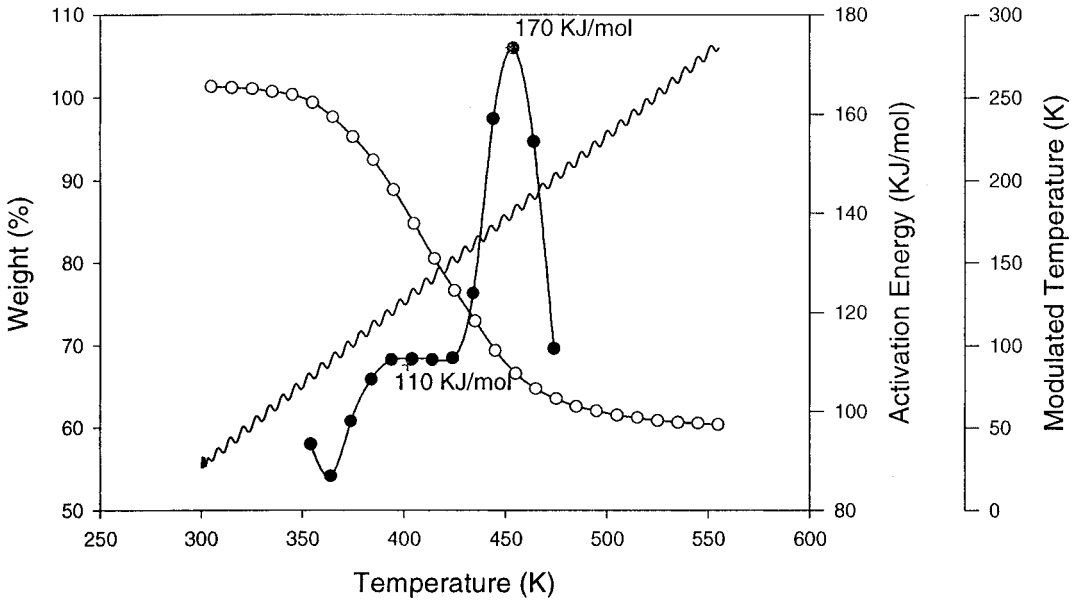

Figure 13. Modulated TGA plot showing the thermogram (○), activation energy (●) and temperature modulations (—).

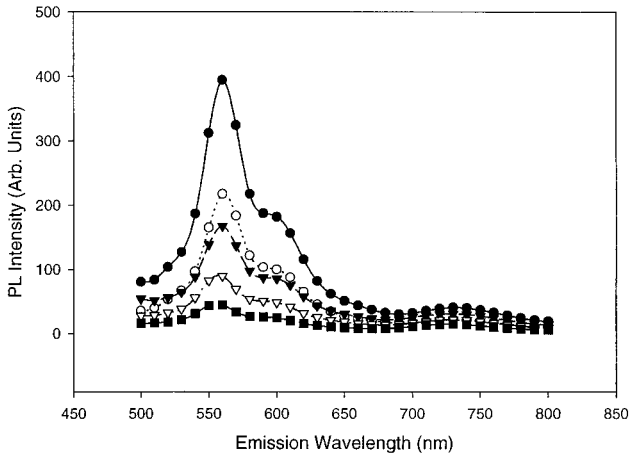

Figure 14. Photoluminescence spectra of PPV films converted with different heating rates and different inert atmosphere: (●) 5 K/min in forming gas, (○) 10 K/min in forming gas, (▼) 5 K/min in nitrogen, (▽) 20 K/min in forming gas, and (■) 10 K/min in nitrogen.

Because no increase in carbonyl defects is observed when only the heating rate is changed while keeping the reaction atmosphere the same, it is not clear whether the lower concentration of carbonyl defects is responsible for improved luminescence at slower heating rates or some other thermodynamic factors or morphological effects are involved. However, it can be safely concluded that if carbonyl defects are indeed responsible for the above effect, then the change in its concentration is too small to be observed spectroscopically.

5. Conclusions

The thermal elimination reaction in the PPV precursor is fairly complex. We have shown that both E1 and E2 mechanisms may be operative on the basis of the reaction temperature. This explains previous conflicts in the literature. This conclusion was possible because we combined several thermoanalytical techniques which provided an understanding of the underlying processes, their chronology, and the mechanism involved. We have also used these thermal techniques to approximate kinetic parameters such as activation energy and half-life from the computational analysis of the results. The half-life approximation is of importance where storage of the PPV precursor may be of practical necessity. Finally, the conditions of the thermal elimination reaction have been found to influence the photoluminescence in the final PPV. Thus, an enhanced understanding of the thermal elimination reaction which converts the precursor to PPV as presented herein will be useful in the many applications of this fascinating polymer.

Acknowledgment. Financial support from NSF YI DMR92-58167 and NSF CHE96-01710-ARI are gratefully acknowledged. G.A.A. also appreciates an Alfred P. Sloan Research Fellowship. Assistance from John Flynn at TA Instruments for arranging the MTGA experiment and for providing the kinetics software is also greatly appreciated. The authors also acknowledge the Chemistry Department at Princeton University for the use of the PL spectrophotometer.

References and Notes

(1) Murase, I.; Ohnishi, T.; Noguchi, T.; Hirooka, M. *Synth. Met.* **1987**, *17*, 639.
(2) Pichler, K. *Philos. Trans. R. Soc. London, Ser. A* **1997**, *355*, 829.
(3) Burroughes, J. H.; Bradley, D. D. C.; Brown, A. R.; Marks, R. N.; Mackay, K. D.; Friend, R. H.; Burn, P. L.; Holmes, A. B. *Nature* **1990**, *347*, 539.
(4) Antoniadis, H.; Hsieh, B. R.; Abkowitz, M. A.; Jenekhe, S. A.; Stolka, M. *Synth. Met.* **1994**, *62*, 265.
(5) Burn, P. L.; Bradley, D. D. C.; Friend, R. H.; Brown, A. R.; Holmes, A. B. *Synth. Met.* **1991**, *41*, 261.
(6) Papadimitrakopoulos, F.; Yan, M.; Rothberg, L. J.; Katz, H. E.; Chandross, E. A.; Galvin, M. *Mol. Cryst. Liq. Cryst. Sci. Technol.* **1994**, *256*, 663.
(7) Papadimitrakopoulos, F.; Konstadinidis, K.; Miller, T. M.; Opila, R.; Chandross, E. A.; Galvin, M. E. *Chem. Mater.* **1994**, *6*, 1563.
(8) Lenz, R. W.; Han, C.; Stenger-Smith, J.; Karasz, F. E. *J. Polym. Sci. Part A: Polym. Chem.* **1988**, *26*, 3241.
(9) Papadimitrakopoulos, F.; Haddon, R. C.; Yan, M.; Miller, T. M.; Rothberg, L. J.; Katz, H. E.; Galvin, M. E. *Polym. Mater. Sci. Eng.* **1995**, *72*, 455.
(10) Rothberg, L. J.; Yan, M.; Papadimitrakopoulos, F.; Galvin, M. E.; Kwock, E. W.; Miller, T. M. *Synth. Met.* **1996**, *80*, 41. (b) Hsieh, B. R.; Antoniadis, H.; Abkowitz, M. A.; Stolka, M. *Polym. Prepr.* **1992**, *33* (2), 414.
(11) Karasz, F. E.; Gagnon, D. R.; Capistran, J. D.; Lenz, R. W. *Mol. Cryst. Liq. Cryst. Sci. Technol.* **1985**, *118*, 327.

(12) Massardier, V.; Hoang, T.; Guyot, A. *Polym. Adv. Technol.* **1994**, *5*, 656.
(13) Halliday, D. A.; Burn, P. L.; Friend, R. H.; Holmes, A. B. *J. Chem. Soc., Chem. Commun.* **1992**, 1685.
(14) Schlenoff, J. B.; Wang, L. *Macromolecules* **1991**, *24*, 6653.
(15) Shah, H. V.; McGhie, A. R.; Arbuckle, G. A. *Thermochim. Acta* **1996**, *287*, 319.
(16) Ezquerra, A. T.; Lopez-Cabarcos, E.; Baltà-Calleja, F. J.; Stenger-Smith, J. D.; Lenz, R. W. *Synth. Met.* **1991**, *41*, 269.
(17) Antoun, S.; Karasz, F. E.; Lenz, R. W. *J. Polym. Sci., Part A: Polym. Chem.* **1988**, *26*, 1809.
(18) Gagnon, D. R.; Capistran, J. D.; Karasz, F. E.; Lenz, R. W.; Antoun, S. *Polymer* **1987**, *28*, 567.
(19) ASTM E1641-94. *Annu. Book ASTM Stand.* Test Method for Decomposition Kinetics by Thermogravimetry. 1994, Vol. 14.02.
(20) Doyle, C. D. *J. Appl. Polym. Sci.* **1961**, *5*, 285.
(21) Flynn, J. H.; Wall, L. A. *Polym. Lett.* **1966**, *4*, 323.
(22) Flynn, J. H. *Thermal Analysis, Vol. 2*. Schwenker, R. F., Garn, P. D., Eds.; Academic Press: New York, 1969.
(23) Blaine, R. *Am. Lab.* **1998**, *30*, 21.
(24) Blaine, R. *Proc. 24th N. Am. Therm. Anal. Soc. Conf.* Morgan, R., Ed.; McLean: Virginia, 1997.
(25) Wessling, R. A.; Zimmerman, R. G. U.S. Patent *3,401,152*, 1968.
(26) Wessling, R. A. *J. Polym. Sci: Polym. Symp.* **1985**, *72*, 55. (b) Burn, P. L.; Kraft, A.; Baigent, D. R.; Bradley, D. D. C.; Brown, A. R.; Friend, R. H.; Gymer, R. W.; Holmes, A. B.; Jackson, R. W. *J. Am. Chem. Soc.* **1993**, *115*, 10117. (c) Hsieh, B. R. *The Polymeric Materials Encyclopedia*, Vol. 9; Salamone, J. C., Ed.; CRC Press Boca Raton, FL, 1996; pp 6537−48. (d) Son, S.; Dodabalapur, A.; Lovinger, A. J.; Galvin, M. E. *Science* **1995**, *269*, 376.
(27) Sykes, P. *A Guidebook to Mechanisms in Organic Chemistry*; Longman: New York, 1982. (b) Sykes, P. *The Search for Organic Reaction Pathways*; Wiley: New York, 1972. (c) March, J. *Advanced Organic Chemistry*; Wiley: New York, 1992.
(28) Garay, R. O.; Baier, U.; Bubeck, C.; Müllen *Adv. Mater.* **1993**, *5*, 561.

MA981108Q